TECHNICAL ARTICLE

Certification of Standard Reference Material 1976B

David R. Black,[a] Donald Windover, Marcus H. Mendenhall, Albert Henins, James Filliben, and James P. Cline
National Institute of Standards and Technology, Gaithersburg, Maryland 20899

(Received 14 January 2015; accepted 30 April 2015)

The National Institute of Standards and Technology (NIST) certifies a suite of Standard Reference Materials (SRMs) to address specific aspects of the performance of X-ray powder diffraction instruments. This report describes SRM 1976b, the third generation of this powder diffraction SRM. SRM 1976b consists of a sintered alumina disc, approximately 25.6 mm in diameter by 2.2 mm in thickness, intended for use in the calibration of X-ray powder diffraction equipment with respect to line position and intensity as a function of 2θ-angle. The sintered form of the SRM eliminates the effect of sample loading procedures on intensity measurements. Certified data include the lattice parameters and relative peak intensity values from 13 lines in the 2θ region between 20° and 145° using Cu$K\alpha$ radiation. A NIST-built diffractometer, incorporating many advanced and unique design features was used to make the certification measurements. © *2015 International Centre for Diffraction Data.*
[doi:10.1017/S0885715615000445]

Key words: Standard Reference Material, X-ray diffraction, certification, lattice parameter, diffractometer

I. INTRODUCTION

The need for a line intensity standard was established by a round robin study pursued through the International Centre for Diffraction Data, ICDD (Jenkins, 1992). The round robin evaluated instruments in the field with respect to diffraction intensity as a function of 2θ angle, or instrument sensitivity. The observed variations in instrument sensitivity were sufficiently large that they would preclude continued improvement of the ICDD database. However, with a suitable National Institute of Standards and Technology (NIST) Standard Reference Material (SRM) these variations could be quantified and corrected through conventional, single peak data analyses methods, and thereby not limit further development of the database. Since its original certification in 1991, this SRM has been adopted by several instrument vendors for verification of proof-of-performance of instruments in the field and is now the largest selling of the NIST SRMs for powder diffraction.

II. MATERIAL

The sintered alumina discs that make up the feedstock for SRM 1976b were prepared for NIST with a dedicated processing run by International Business Machines Corporation (Certain commercial equipment, instruments, or materials are identified in order to adequately specify the experimental procedure. Such identification does not imply recommendation or endorsement by the National Institute of Standards and Technology, nor does it imply that the materials or equipment identified are necessarily the best available for the purpose.). While the manufacturing process itself is proprietary, an examination of the microstructure in conjunction with the ceramic engineering background of one the authors leads to general conclusions about the manufacturing method that was used. The alumina powder precursor material consisted of a "tabular" alumina powder that had been calcined to a high temperature, approximately 1500 °C. This calcination results in a phase-pure alpha alumina powder with a plate-like crystal morphology. The single-crystal platelets are nominally 10 μm in diameter by 2–3 μm in thickness. The compacts were liquid phase sintered using a 3–5% anorthite glass matrix with hot forging being used to achieve a compact of approximately 97% theoretical density. Owing to the pressing operation and the plate-like morphology of crystals, the basal planes preferentially oriented parallel to the sample surface during manufacture. This results in the SRM displaying a moderate level of crystallographic texture, with the *c*-axes orientated to a multiple-of-a-random-distribution of the order of 5 with respect to the surface normal. However, a unique outcome of the hot forging operation was that the texture imparted to the microstructure is axisymmetric, permitting the mounting of the sample in any orientation about the surface normal.

Other desirable aspects of the microstructure of SRM 1976b include the near absence of sample-induced profile broadening. The crystallites are large enough that size broadening is not observed and strain broadening is minimized by the relaxation of the anorthite glass matrix during cooling. As the sintered compacts cool, the viscosity of anorthite steadily increases, solidifying at approximately 800 °C. This allows for intergranular movement during cooling, at least until 800 °C, which reduces the level of micro-strain that would otherwise build between the grains because of the anisotropic thermal expansion of alumina. However, SRM 1976b still displays a slight but discernable level of Gaussian micro-strain broadening. Given this, and the essential absence of crystallite

[a]Author to whom correspondence should be addressed. Electronic mail: david.black@nist.gov

size broadening, SRM 1976b can be used to obtain an approximation of the instrument profile function (IPF). Use of SRM 1976b is not recommended; however, for quantitative microstructure analyses. The nominally 25.6 mm discs of SRM 1976b were stamped from a sheet during manufacturing, this resulted in the edge of the disc surface being depressed by approximately 10 μm relative to the center. This is not regarded as a significant difficulty because of the low attenuation of X-rays by alumina; nonetheless, height justification during mounting should be with respect to the center of the disc.

III. INSTRUMENTATION AND DATA COLLECTION

Certification was performed using data from a NIST-built diffractometer that can be converted between several optical configurations. The goniometer assembly is exceedingly stiff and fully encoded to provide accurate angle measurement. The optical components were obtained from commercial diffraction equipment. Two divergent beam, Bragg–Brentano configurations were used in the certification of SRM 1976b. Lattice parameters were measured using data from conventional, slit-based incident, and receiving optics that included a graphite monochromator located between the sample and detector, a post-monochromator. The data for the certified relative intensities were collected with the machine equipped with a Johansson incident beam monochromator (IBM). The IBM simplifies the IPF such that the observed profiles can be accurately fit using analytical profile shape functions (PSFs). The instrument is described by Black *et al*. (2011) and more recently by Cline *et al*. (2013); the latter reference includes a discussion of the IBM. A most complete discussion of the machine and the procedures used for its alignment and qualification are discussed by Cline *et al*. (2015).

When the diffractometer was set up with the post-monochromator, a 2.2 kW sealed copper tube of long fine-focus geometry was operated at a power of 1.8 kW during certification measurements. The nominal source size was 12 mm × 0.04 mm. Axial divergence of the incident beam was limited by a 2.2° Soller slit. Scattered X-rays were filtered with a graphite post-sample monochromator, and counted with a scintillation detector. In the case of the Johansson IBM, a 1.6 kW copper tube of fine-focus geometry was used and operated at a power of 1.2 kW during certification measurements. The nominal source size was 8 mm × 0.04 mm. In this case a 2.2° Soller slit was used in the receiving optics to limit axial divergence. Common to both configurations was the use of a variable divergence slit which was set nominally to 0.8°. Also, a 2 mm anti-scatter slit was placed approximately 113 mm in front of the 0.2 mm (0.05°) receiving slit. The goniometer radius was 217.5 mm. Samples were spun at 0.5 Hz during data collection. The diffractometer was located within a temperature-controlled laboratory space where the nominal short-range control of temperature was ±0.1°K. The instrument was controlled via LabVIEW software and data were recorded in true *x*–*y* format using the reading from the encoder as the recorded angle. The source was allowed to equilibrate at operating conditions for at least 1 h prior to recording any certification data. The performance of the machine was qualified with the use of NIST SRM 660b Line Position and Line Shape Standard for Powder Diffraction (SRM 660b, 2009) and SRM 676a Alumina Powder for Quantitative Analysis by X-ray diffraction (SRM 676a, 2008) using procedures discussed by Cline *et al*. (2013) and Cline *et al*. (2015).

Twenty units of SRM 1976b were selected in a stratified random manner from the population of units being certified. Diffraction data used for the determination of certified relative intensities were collected in a single continuous scan using a 2θ range from 20° to 160°, with a step width of 0.008° and a count time of 4 s per step. This resulted in a total collection time of approximately 24 h per sample. A graphical evaluation of the intensity values from the 104 reflection of each sample indicated no systematic degradation of the tube performance over the course of data collection. The data used for the determination of certified lattice parameters were collected from 11 selected regions; run time parameters for each region were adjusted with regards to observed full-width at half-maximum (FWHM) and diffraction intensity to optimize data quality per unit time. Five of the regions contained one profile, the remainder contained from three to six profiles and this accessed all the reflections with a relative intensity greater than approximately 2.0% within the 2θ range of 20°–154°. The angular widths of the scan ranges were 20–30 times the observed FWHM values of the profiles and were chosen to provide at least 0.3° 2θ of apparent background straddling each peak. The step width was chosen to include at least eight data points above the FWHM. The count time for each profile was inversely proportional to the observed diffraction intensity to provide constant counting statistics among the profiles. Again, the total collection time was approximately 24 h per sample.

IV. DATA ANALYSIS

The measurands to be certified in SRM 1976b consist of the lattice parameters and the 13 relative intensity values. The certified lattice parameters were determined using the fundamental parameters approach (FPA) (Cheary and Coelho, 1992) within a Rietveld analysis (Rietveld, 1967, 1969). The data for this were collected using optics that would not significantly distort the emission spectrum of the Cu$K\alpha$ radiation from that expected from a naked beam. This permitted the use of the emission spectrum as characterized by Hölzer *et al*. (1997) to construct the diffraction profiles as per the FPA, ensuring a robust SI traceability of the certified lattice parameters. The second measurand, the 13 relative intensity values, is affected by the level of texture displayed by the SRM feedstock. However, the precise degree of texture is immaterial, what is critical is the uniformity in the texture levels from sample to sample. To minimize this, the feedstock for SRM 9176b was prepared with a dedicated processing run. Any lack of uniformity in texture would manifest itself as an increase in the uncertainty associated with the certified relative intensity values. Therefore the texture of SRM 1976b was not rigorously characterized in the certification.

Analyzing data to determine accurate relative intensity values can be problematic due to the complexities of the line shape observed in laboratory equipment and difficulties in determining the background level. Both of these difficulties were addressed with the use of an IBM in data collection; the profile shape is dramatically simplified and the number of contributions to the background is mitigated. The method used in data analysis was to consider several approaches and software packages until essential agreement between them was realized; lending credibility to the final result. Data for the

https://doi.org/10.1017/S0885715615000445 Published online by Cambridge University Press

certification of relative intensities were analyzed with profile fitting using analytical PSFs, a Rietveld analysis wherein the observed structure factors were extracted, and a NIST-developed tail-weighted fitting (TWF) peak localization method. Two PSFs were used with two commercial X-ray diffraction data analysis packages. The first utilized the split Pearson VII PSF as implemented within TOPAS (2009), whereas the second used the split Voigt PSF as implemented within HighScore Plus (HighScore). The Rietveld analyses were done via GSAS (Larson and Von Dreele, 2003).

The NIST-developed method consists of profile fitting using a symmetric Voigt PSF with a two-step process the first of which involves fitting with a weighting function that biases the fit toward the tail regions of the PSF. This approach mitigates the difficulty in determining accurate areas in the presence of long, Lorentzian tails. Owing to the length of the Lorenztian tails of the Voigt PSF, cutting off a peak shape function too early results in a fit in which the background function is adjusted to compensate for missing tails. Also, inaccuracies in the peak shape model function relative to the actual peak shape will distort the tails to attain a least-squares fit. These problems are addressed by choosing a statistical weighting function in the fit procedure, which forces strong agreement at low intensity (in the tails) at the expense of poor agreement at the top of the peak (where the fit is quite sensitive to the shape function). The weighting function is essentially a constant-relative-error weight merged into a Poisson weight and constant at low counts. Thus, $w = 1/(n_0 + n + \boldsymbol{\alpha}^2\boldsymbol{n}^2)$, where $\boldsymbol{n}$ is the number of counts, n_0 is a small constant (typically 5) to avoid problems, where there might be empty channels, and α is the relative error, typically 10% (0.1). The residual errors from such a fit can be quite substantial in the region of high intensity, but go to zero very quickly as one moves away from the center of a peak, since the tails are fit very accurately. One can then compute the analytical area of the PSF, and add it to the area computed directly from summing the residuals, to get an accurate estimate of the peak area.

With the execution of all methods the background was represented by a tenth-order shifted Chebyshev polynomial. With both of the profile fitting analyses using commercial codes, two shape and two FWHM parameters were refined for each split PSF. The refined parameters of the Rietveld analyses included the scale factors, lattice parameters, sample shift and transparency terms, structural parameters, and the "type 1" Lorentz-Polarization factor. Texture effects were modeled using a sixth-order spherical harmonic. Profile shape was modeled with a Thompson–Cox–Hastings (Thompson *et al*., 1987) "type 3" function using the GU, GW, and LY terms to represent instrumental, crystallite size, and strain broadening. The Finger (Finger *et al*., 1994) model was used to fit profile asymmetry where one of the peak asymmetry parameters, S/L, was refined, while the second, H/L, was fixed such that the two terms were nearly equal. Relative intensities were extracted with the GSAS utility REFLIST, which uses the observed structure factors, corrected for multiplicity and Lorentz-polarization factor, to compute relative intensity values. The observed structure factors are determined from a background subtracted summation of the counts in the peak region of the raw data. No PSF is used. The Rietveld analysis served only to fit the background, determine the peak cut-off angles, and the ratio of the intensity distributed between overlapping lines.

TABLE I. Average relative intensity values for each data analysis method.

Reflection (*hkl*)	Split Voigt PSF	Split Pearson VII PSF	GSAS	NIST TWF
(012)	23.82	23.71	23.68	23.44
(104)	100.00	100.00	100.00	100.00
(113)	37.27	37.15	37.33	36.89
(024)	20.91	20.86	21.05	20.77
(116)	87.42	87.13	87.79	87.01
(300)	12.56	12.43	12.63	12.36
(1.0.10) & (119)	70.40	70.50	71.20	69.28
(0.2.10)	13.17	13.05	13.27	12.93
(226)	8.11	8.00	8.17	8.05
(2.1.10)	16.25	16.09	16.32	16.00
(324) & (0.1.14)	25.48	24.94	25.46	24.30
(1.3.10)	14.83	14.58	14.86	14.39
(146)	12.86	12.42	12.68	12.35
(4.0.10)	11.35	10.69	11.04	11.36

The intensity data from the four methods are listed in Table I. Certification data are reported only from the Rietveld analyses as these are judged most accurate because a profile shape model is not used. Figure 1 illustrates the discrepancies between the relative intensity values determined from the use of the observed structure factors via GSAS relative to the results from the profile fitting methods. With use of the split Voigt PSF, deviations are generally <1% negative for all but the high angle lines where it approaches a value 3% larger than the certified values. In the case of the split Pearson VII PSF, the discrepancies are more systematically negative with the deviations increasing with 2θ, to a maximum value at high angle of about 3% below the certified values. Nonetheless, the commonality of these data served to validate the results. The certified relative intensities of SRM 1976b and their expanded uncertainties, using the $k = 2$ factor, are shown in Table II. Such uncertainty values represent our degree of confidence in the reported relative intensity values in the absence of systematic error (ISO, 1993; Taylor, 1995).

The certification data for lattice parameters were analyzed using the FPA method with a Rietveld refinement as implemented in TOPAS. The analysis used the Cu$K\alpha$ emission spectrum, including a satellite component, as characterized by Hölzer *et al*. (1997) and Maskil and Deutsch (1988). Hölzer models the Cu$K\alpha_1$/$K\alpha_2$ doublet using four Lorentzian profiles, two primary ones, $K\alpha_{11}$ and $K\alpha_{21}$, and two secondary ones, $K\alpha_{12}$ and $K\alpha_{22}$ where the latter two are of reduced intensity and only serve to account for the asymmetry observed in the spectrum. During calibration of the instrument, using the highest quality data from SRM 660b, the four Lorentzian breadths of the Cu emission spectrum were refined with constraints to preserve the asymmetric profile shape as modeled by Hölzer. This analysis also accounted for the reduction in the FWHM values of the emission spectrum because of the non-uniform band-pass of the graphite monochromator to yield an appropriate set of breadths.

The refined parameters for the certification data included the wavelengths and intensities of the $K\alpha_2$ and satellite lines, the scale factors, second-order Chebyshev polynomial terms for modeling of the background, the lattice parameters, terms indicating the position and intensity of the "tube tails" (Bergmann *et al*., 2000), a Soller slit value in the "full"

https://doi.org/10.1017/S0885715615000445 Published online by Cambridge University Press

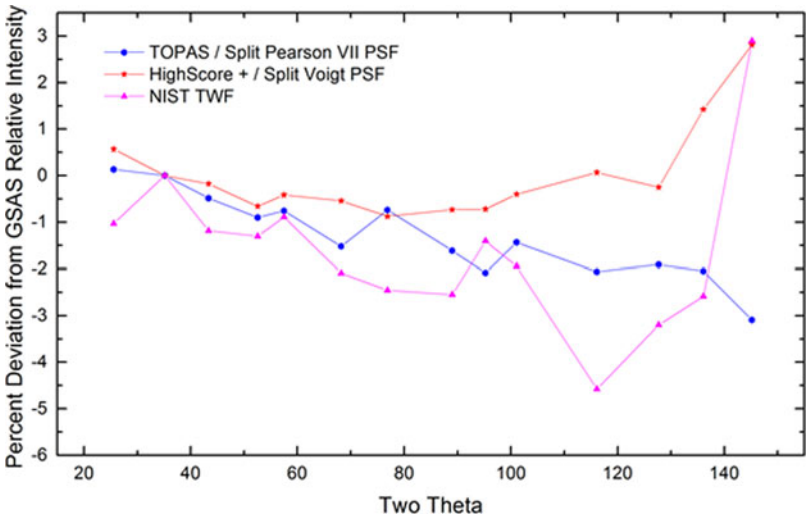

Figure 1. (Color online) Deviations in relative intensity values obtained from profile fitting compared with those obtained from the observed structures factors via GSAS.

axial divergence model (Cheary and Coelho, 1998*a*, *b*) as the axial divergence of the incident and diffracted beams was constrained to be identical, specimen displacement, an attenuation term, structural parameters, a crystallite size broadening term of a Lorentzian profile, and a micro-strain broadening term of a Gaussian profile. Texture effects were modeled with a sixth-order spherical harmonic.

Examination of the fit to individual profiles revealed a discrepancy between the model and the observations in the low-angle region. It is well known that low-angle profiles are more prone to error than high-angle lines as the optical aberrations affecting their position are more complex. Also, the lattice parameter is more strongly affected by angular errors in the low-angle region. The 012 line was, therefore, not used in obtaining the certified lattice parameters. The thermal expansion of alumina as reported by Shvyd'ko *et al*. (2002) was used to adjust the lattice parameter to 22.5 °C. A statistical analysis of the data indicated that the means of the measurements were $a = 0.475\,913\,67$ nm and $c = 1.299\,337\,2$ nm with a $k = 2$ Type A expanded uncertainty of 0.000 000 66 nm and 0.000 001 1 nm for a and c, respectively. However, a Type B uncertainty because of systematic error must be incorporated into the uncertainty bounds of the certified lattice parameter. An examination of the uniformity in the computed lattice parameter as a function of 2θ leads to an assignment of a Type B uncertainty that is roughly an order of magnitude larger than the Type A. The certified lattice parameters and their expanded uncertainties, Type A compounded with Type B, are shown in Table III. Peak positions were computed from the certified lattice parameters and are shown in Table IV as ancillary data.

Diffraction intensity data were recorded with the diffractometer equipped with an IBM. The use of SRM 1976b for the calibration of X-ray diffraction equipment of differing optical configurations will require that a bias be applied to the certified intensity values. This bias is needed to account for differences in the polarization effects from the presence, absence, and character of crystal monochromators. The polarization factor for a diffractometer that is not equipped with a monochromator is, from Guinier (1994):

$$\frac{1 + \cos^2 2\theta}{2}. \tag{1}$$

The polarization factor for a diffractometer equipped with only an IBM is, from Azaroff (1955):

$$\frac{1 + \cos^2 2\theta_m \cos^2 2\theta}{1 + \cos^2 2\theta_m}, \tag{2}$$

where $2\theta_m$ is the 2θ angle of diffraction from the monochromator crystal. The polarization factor for a diffractometer equipped with only a diffracted beam, post-monochromator is, from Yao and Jinno (1982):

$$\frac{1 + \cos^2 2\theta_m \cos^2 2\theta}{2}, \tag{3}$$

where, again, $2\theta_m$ is the 2θ angle of the monochromator crystal. Eqs. (2) and (3) are considered appropriate when the monochromator crystal is of an "ideal mosaic" structure, i.e. the diffracting domains are uniformly small and, therefore,

TABLE II. Certified relative intensity data from SRM 1976b.

Reflection (*hkl*)	Relative intensity	Expanded uncertainty ($k = 2$)
(012)	23.68	±0.21
(104)	100	–
(113)	37.33	±0.25
(024)	21.05	±0.20
(116)	87.79	±0.49
(300)	12.63	±0.20
(1.0.10) & (119)	71.2	±0.63
(0.2.10)	13.27	±0.12
(226)	8.17	±0.07
(2.1.10)	16.32	±0.13
(324) & (0.1.14)	25.46	±0.28
(1.3.10)	14.86	±0.12
(146)	12.68	±0.08
(4.0.10)	11.04	±0.14

TABLE III. Certified lattice parameters of SRM 1976b.

	Lattice parameter (nm)	Expanded uncertainty ($k = 2$)
a	0.475 913 7	±0.000 008 0
c	1.299 337	±0.000 015

https://doi.org/10.1017/S0885715615000445 Published online by Cambridge University Press

TABLE IV. Ancillary peak position data for SRM 1976b, lines listed with a relative intensity >5%, computed using Cu$K\alpha$ radiation, $\lambda = 0.154\,059\,29$ nm.

Reflection (*hkl*)	Peak position (2θ, degrees)
(012)	25.575
(104)	35.147
(110)	37.775
(006)	41.673
(113)	43.351
(024)	52.548
(116)	57.495
(018)	61.297
(214)	66.515
(300)	68.207
(1.0.10)	76.866
(119)	77.229
(0.2.10)	88.989
(0.0.12)	90.699
(226)	95.242
(2.1.10)	101.066
(324)	116.091
(0.1.14)	116.588
(1.3.10)	127.669
(3.0.12)	129.862
(2.0.14)	131.083
(146)	136.063
(1.1.15)	142.292
(4.0.10)	145.152
(1.2.14)	150.081
(1.0.16)	150.38
(330)	152.402

the crystal is diffracting in the kinematic limit. This is in contrast to a "perfect" crystal, which would diffract in accordance with dynamical scattering theory. Note that Eqs. (2) and (3) both have the $\cos^2 2\theta_m$ multiplier operating on the $\cos^2 2\theta$ term. Since this multiplier is less than unity, machines equipped with a monochromator exhibit a weaker angular dependence.

The simplified IPF of the NIST instrument as configured with an IBM and scintillation detector is advantageous for the accurate fitting of the profiles and, therefore, intensity measurement. The validity of the "ideal mosaic" assumption embodied in Eq. (2) was evaluated using this diffractometer and the validity of Eq. (3) was evaluated with the machine configured with the post-monochromator. The IBM used a Ge crystal (111) reflection and $2\theta_m$ was set to 27.3°. The post-sample monochromator used a pyrolytic graphite crystal (0002) basal plane reflection and $2\theta_m$ was set to 26.6°. Rietveld analyses of data from SRMs 660b, 1976b, and 676a, which included a refinement of the polarization factor, modeled as per Eqs. (2) and (3) in *TOPAS*, yielded fits of high quality, indicating that these models were appropriate for these crystals and configurations. Eqs. (1)–(3) were used to bias the certified values to correspond to those of alternative configurations. These values are included in Table V as ancillary data. The user may select the set of relative intensity values from Table V that are appropriate for the configuration of the instrument to be qualified and proceed accordingly. Use of SRM 1976b for additional configurations may require computation of biases alternative to those presented herein.

TABLE V. Ancillary biased relative intensity data for SRM 1976b.

Reflection (*hkl*)	Relative intensity	
	No monochromator	Graphite post-monochromator
(012)	23.95	23.67
(104)	100	100
(113)	36.87	37.36
(024)	20.43	21.08
(116)	84.37	88.02
(300)	11.86	12.68
(1.0.10) & (119)	65.72	71.37
(0.2.10)	12.15	13.34
(226)	7.49	8.21
(2.1.10)	15.04	16.4
(324) & (0.1.14)	24.14	25.55
(1.3.10)	14.44	14.89
(146)	12.51	12.69
(4.0.10)	11.04	11.04

V. CONCLUSION

A NIST-built divergent beam diffractometer, incorporating many advanced design features, has been used to certify the lattice parameters and relative peak intensities of alumina for SRM 1976b. The alumina powder was specifically prepared to minimize the effects of strain broadening. It was compacted into discs with axisymmetric texture to eliminate variations because of sample mounting procedures. Both Type A, statistical, and Type B, systematic, errors have been assigned to yield certified values for the lattice parameters of $a = 0.475\,913 \pm 0.000\,008\,0$ nm and $c = 1.299\,337 \pm 0.000\,015$ nm. The intensity of diffraction peaks with an intensity > 8% of that of the (104) peak have been certified. The instrument was configured with an IBM for these measurements. Biased intensity data appropriate for different optical configurations is provided as ancillary data.

Azaroff, L. V. (**1955**). "Polarization correction for crystal-monochromatized x-radiation," Acta Crystallogr. **8**, 701–704.

Bergmann, J., Kleeberg, R., Haase, A., and Breidenstein, B. (**2000**). "Advanced Fundamental Parameters Model for Improved Profile Analysis," in *Proc. of the 5th European Conf. on Residual Stresses, Delft-Noordwijkerhout, The Netherlands, September 29–30, 1999*, edited by A. J. Böttger, R. Delhez and E. J. Mittemeijer (Material Science Forum), Vol. **347–349**, pp. 303–308.

Black, D. R., Windover, D., Henins, A., Filliben, J., and Cline, J. P. (**2011**). "Certification of standard reference material 660B," Powder Diffr. **26** (2), 155–158.

Cheary, R. W. and Coelho, A. A. (**1992**). "A fundamental parameters approach to X-ray line-profile fitting," J. Appl. Crystallogr. **25**, 109–121.

Cheary, R. W. and Coelho, A. A. (**1998a**). "Axial divergence in a conventional x-ray powder diffractometer I. theoretical foundations," J. Appl. Crystallogr. **31**, 851–861.

Cheary, R. W. and Coelho, A. A. (**1998b**). "Axial divergence in a conventional x-ray powder diffractometer II. implementation and comparison with experiment," J. Appl. Crystallogr. **31**, 862–868.

Cline, J. P., Black, D., Windover, D., and Henins, A. (**2013**). "The Calibration of Laboratory X-Ray Diffraction Equipment Using NIST Standard Reference Materials, Chapter 13," in *Modern Diffraction Methods*, edited by E. J. Mittemeijer and U. Welzel (Wilcy-VCH, Weinheim, Germany), pp. 399–438.

Cline, J. P., Mendenhall, M. H., Black, D., Windover, D., and Henins, A. (**2015**). "The optics, alignment and calibration of laboratory X-ray powder diffraction equipment with the use of NIST standard reference materials," *Int. Tables Crystallogr. H: Powder Diffraction*, in press.

https://doi.org/10.1017/S0885715615000445 Published online by Cambridge University Press

Finger, L. W., Cox, D. E., and Jephcoat, A. P. (**1994**). "A correction for powder diffraction peak asymmetry due to axial divergence," J. Appl. Crystallogr. **27**, 892–900.

Guinier, A. (**1994**). *X-Ray Diffraction in Crystals, Imperfect Crystals, and Amorphous Bodies* (Courier Dover Publications, N. Chelmsford, Massachusetts).

HighScore Plus. *V3.0d PANalytical* (BV Almelo, The Netherlands).

Hölzer, G., Fritsch, M., Deutsch, M., Härtwig, J., and Förster, E. (**1997**). "$K\alpha_{1,2}$ and $K\beta_{1,3}$ x-ry emission lines of the 3d transition metals," Phys. Rev. A **56**(6), 4554–4568.

ISO (**1993**). *Guide to the Expression of Uncertainty in Measurement; ISBN 92-67-10188-9* (International Organization for Standardization, Geneva, Switzerland), 1st ed.

Jenkins, R. (**1992**). Round Robin on Powder Diffractometer Sensitivity; ICDD Workshop at the Conference Accuracy in Powder Diffraction II; NIST Gaithersburg, May 26–29.

Larson, A. C. and Von Dreele, R. B. (**2003**). *General Structure Analysis System (GSAS); Report LAUR 86–748* (Los Alamos National Laboratory, Los Alamos, New Mexico).

Maskil, M. and Deutsch, M. (**1988**). "X-ray Kα satellites of copper," Phys. Rev. A **38**, 3467–3472.

Rietveld, H. M. (**1967**). "Line profiles of neutron powder-diffraction peaks for structure refinement," Acta Crystallogr. **22**, 151–152.

Rietveld, H. M. (**1969**). "A profile refinement method for nuclear and magnetic structures," J. Appl. Crystallogr. **2**, 65–71.

Shvyd'ko, Yu. V., Lucht, M., Gerdaua, E., Lerche, M., Alp, E. E., Sturhahn, W., Sutter, J., and Toellner, T. S. (**2002**). "Measuring wavelengths and lattice constants with the mossbauer wavelength standard," J. Synchr. Radiat. **9**, 17–23.

SRM 660b (**2009**). *Line Position and Line Shape Standard for Powder Diffraction* (National Institute of Standards and Technology; U.S. Department of Commerce, Gaithersburg, MD).

SRM 676a (**2008**). *Alumina Internal Standard for Quantitative Analysis by Powder Diffraction* (National Institute of Standards and Technology; U.S. Department of Commerce, Gaithersburg, MD).

Taylor, B. N. (**1995**). *Guide for the Use of the International System of Units* (SI) (NIST Special Publication 811; U.S. Government Printing Office, Washington, DC).

TOPAS. (**2009**). *General Profile and Structure Analysis Software for Powder Diffraction Data*, V4.2, (Bruker AXS GmbH, Karlsruhe, Germany).

Thompson, P., Cox, D. E., and Hastings, J. B. (**1987**). "Rietveld refinement of Debye-Scherrer synchrotron X-ray data from Al_2O_3," J. Appl. Crystallogr. **20**, 79–83.

Yao, T. and Jinno, H. (**1982**). "Polarization factor for the X-ray powder diffraction method with a single crystal monochromator," Acta Crystallogr. A **38**, 287–288.

https://doi.org/10.1017/S0885715615000445 Published online by Cambridge University Press